Research Paper
J. Astron. Space Sci. 41(1), 17-23 (2024)
https://doi.org/10.5140/JASS.2024.41.1.17

JASS Journal of Astronomy and Space Sciences

Simulation and Design of Optimized Three-Layer Radiation Shielding to Protect Electronic Boards of Satellite Revolving in Geostationary Earth Orbit (GEO) Orbit against Proton Beams

Ali Alizadeh, Gohar Rastegarzadeh†
Department of Physics, Semnan University, Semnan 35131-19111, Iran

The safety of electronic components used in aerospace systems against cosmic rays is one of the most important requirements in their design and construction (especially satellites). In this work, by calculating the dose caused by proton beams in geostationary Earth orbit (GEO) orbit using the MCNPX Monte Carlo code and the MULLASSIS code, the effect of different structures in the protection of cosmic rays has been evaluated. A multi-layer radiation shield composed of aluminum, water and polyethylene was designed and its performance was compared with shielding made of aluminum alone. The results show that the absorbed dose by the simulated protective layers has increased by 35.3% and 44.1% for two-layer (aluminum, polyethylene) and three-layer (aluminum, water, polyethylene) protection respectively, and it is effective in the protection of electronic components. In addition to that, by replacing the multi-layer shield instead of the conventional aluminum shield, the mass reduction percentage will be 38.88 and 39.69, respectively, for the two-layer and three-layer shield compared to the aluminum shield.

Keywords: cosmic rays, proton beam, geostationary Earth orbit (GEO) orbit, MCNPX, MULLASSIS

1. INTRODUCTION

Outer space is considered a radiation environment for satellites due to the existence of different rays. The physical and chemical reactions of this environment greatly affect the performance and lifespan of electronic devices and equipment, including memories, transistors, microcontrollers, and microprocessors. Many of these parts and equipment must be strengthened to work in radiation environments. If these devices are not resistant to the radiation environment, they will suffer a lot of damage, which will cause various harmful effects based on the type of radiation, the frequency and the type of radiation interaction. If the amount of these damages is more than the tolerance of the electronic part, that part will fail and in the worst case, all the systems may be disturbed and the project will face a complete failure.

Therefore, it is not possible to guarantee the survival and success of a space system in the environment of space radiation without considering the effects of radiation and reducing them. Since satellites and other space systems are designed to work in the space plasma environment, they are trapped against high-energy particles and are slightly vulnerable. Space radiations caused by solar events or cosmic sources _when they hit and interact with the surface of satellites and spacecraft_ can affect the space system and electrical components in it in several ways (Nwankwo et al. 2020). The three main categories of these effects are total ionizing dose (TID), single event effect (SEE) and damage displacement (DD) (National Academies of Sciences, Engineering, and Medicine 2018; Blachowicz & Ehrmann 2021). Cosmic rays are mainly composed of energetic charged particles. The three natural sources of cosmic rays are: trapped rays, cosmic rays and solar particles. Earth's

Received 10 NOV 2023 **Revised** 04 JAN 2024 **Accepted** 08 JAN 2024
†**Corresponding Author**
Tel: +98-9123773963, E-mail: grastegar@semnan.ac.ir
ORCID: https://orcid.org/0000-0001-9240-7841

magnetic field traps low-energy cosmic rays and solar particles and forms a radiation belt around the earth. Most of the rays trapped in this belt are protons and electrons. High-energy cosmic particles (25 MeV–20 GeV) include all atoms and stars which are created due to the supernova process. Approximately, 88% of cosmic rays are hydrogen, 10% helium and the remaining 2% other heavier atoms. Solar particles consist of two types of radiation, which are: 1) low-energy solar wind particles that are continuously emitted from the sun. 2) Solar particle events (SPE events). These energetic particles have a high flux and can be extremely dangerous for space systems (Tripathi Ram 2011; Rudychev et al. 2023).

It is very important to choose the appropriate radiation reduction method and combine it with the purpose and concept of the mission at the beginning of the design phase. The most known method of environmental reduction is conservation. Obviously, the use of shielding to reduce the environmental effects leads to an increase in the weight and mass of the satellite. Consequently, the design and construction of the shield has always been under the influence of the mass factor and the radiation environment (Daneshvar et al. 2021).

The most common radiation protection for satellites is to add aluminum to reach the desired radiation level. However, in environments such as the geostationary Earth orbit (GEO) orbit where electrons are dominant, thick aluminum walls are not the most efficient radiation shields, because they are able to weaken the secondary X-rays caused by the collision of electrons with matter. As a result, they are not protective. In general, materials with a higher atomic number, such as tantalum, can greatly weaken X-rays, but when used as electron shielding, they create more secondary X-rays and weigh more. They also impose more on the system (Narici et al. 2017; Lei et al. 2023). Today, polyethylene is considered a suitable protection for the space environment due to its high hydrogen surface, low density, ease of use, reasonable price, and since it prevents nuclear fission processes (Xu et al. 2022). There exists another lighter protection shielding called “multi-layer Graded-z” which not only is protective against energetic protons but also works well in electronic environments. The design of these types of shields usually includes three layers. The first layer is a light material to minimize the production of X-rays. This layer, when hitting electrons and due to its low density, weakens the electrons and produces less secondary radiation as well. The second layer is a material with a higher atomic number to maximize the attenuation of the X-rays produced in the first layer. In the third layer, substances with low atomic number are used to weaken the secondary electrons by producing minimum secondary X- rays. In this structure, the material of the middle layer with a high atomic number does not cause the production of secondary X-rays since the electrons in the primary layer are weakened (Arif Sazali et al. 2019; Hussein et al. 2020; Vepsäläinen et al. 2020; Rudychev et al. 2023).

In the design and construction of radiation shields, choosing the appropriate material and thickness of the layers is essential in reducing the dose and optimizing the weight. This requires experimental and computational work. Despite the greater accuracy of the experimental method, using computational and simulation methods can be time-saving and cost-effective since the practical tests demand high expenses, a long time to be implemented and access to space radiation testing laboratories (Rahman et al. 2017; Li et al. 2018; Shoorian et al. 2019).

2. METHODS

The energy and flux of space rays can be provided by using the space environment information system (SPENVIS). SPENVIS is an online software which models the space environment (including cosmic rays, natural radiation belts, energetic solar particles, plasma gas and micro particles) and its effects. In this work, the radiation environment of GEO orbit as a strategic orbit for telecommunication satellites has been investigated. In the modeling of trapped rays, the AP-8 model for protons (Fig. 1), which is a statistical model and covers the radiation belts completely, has been used (Seon et al. 2020; Liu et al. 2022).

One of the powerful tools in the field of dosimetry calculations of all types of ionizing radiation is the MCNPX code. This code is a Monte Carlo beam transfer software that tracks all particles at almost all energies. In this work, Tally F6 of MCNPX code is used to obtain the energy left by the particles and dose calculations. When using this method, if the transport of secondary particles is not considered and they are not included in the mode card, it is regarded to leave the energy of these particles in the place of interaction (Ferrari et al. 2018).

The other software in this field is MULLASSIS, which uses the Geant4 radiation transfer toolbox to simulate particle transfer in one-dimensional flat or spherical shields. This instrument can be used to determine particle attenuation, ionizing radiation dose and non- ionizing dose, and energy deposition at pulse height as a function of material shielding.

However, for better and more convenient use, MULASSIS is available through the SPENVIS website, so that the user can control the Monte Carlo simulation remotely using a

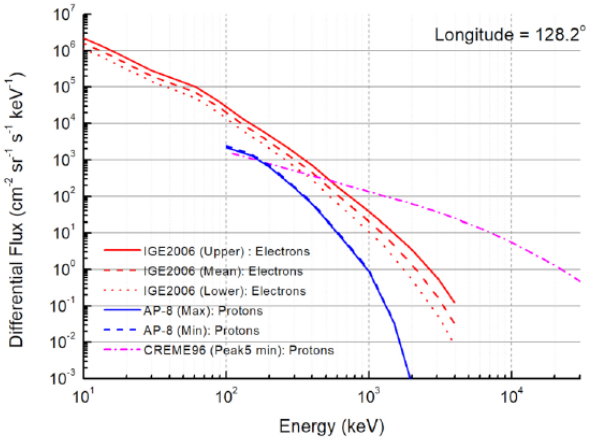

Fig. 1. Average proton and electron fluxes based on models in geostationary orbit. For electron fluxes in geosynchronous orbits, the IGE2006 model is employed, whereas AP-8 is used for proton fluxes. An extreme case of an energetic solar proton event is modeled with the CREME-96 (Peak 5-min) model. Adapted from Sicard-Piet et al. (2008) with CC-BY-NC-ND.

web browser. In the web-based version of the MULASSIS software, the user is presented with a series of web pages that allow him to define geometry and materials used, source particle energy and angular distribution, physical models and particle shear applied, and definition web page analysis requirements. The geometry allows control over the type of geometry (flat or spherical), the number of layers that the shield includes, the thickness of each layer and the composition of the simulated materials.

Therefore, the focus of protection in this work is polyethylene and light elements. In accordance with the points just mentioned and taking the importance of the weight factor in the design of space systems into consideration, this factor has been regarded as one of the criteria for optimizing the thickness of the designed shielding layers in comparison with the aluminum shielding. The conditions of radiation environment for all investigated modes of these shields are considered the same, which include a mission in GEO orbit and is provided by the SPENVIS (Seon et al. 2020). In this work, a multi-layer shield consisting of polyethylene, water and aluminum has been introduced and its performance has been compared with aluminum shield, as the most common radiation shield. Finally, the optimal structure has been selected according to the TID attenuation and shielding mass. The Monte Carlo calculation approach of the MCNPX code and the MULLASSIS code from the Geant4 radiation transfer toolbox have been used to calculate the dose attenuation of various materials in the environment and for a telecommunication satellite with a mission in the GEO space orbit.

The composition of protective layers, whose design is based on the multi- layer structure, is shown in Fig. 2. The first layer is chosen from the outside of polyethylene to minimize the production of X-ray bremsstrahlung. After that, the layer is made of water, so it weakens the braking X-rays produced in the polyethylene layer. Since electronic devices are usually placed in aluminum boxes, it is placed at the end and the innermost layer of aluminum.

The studied satellite protection structure is a cube-shaped structure made of aluminum alloy 7075 made by CUBESAT Company and has known dimensions according to Fig. 3, which is simulated by MCNP software (ISISPACE 2024).

Most of the standard commercial electronic components usually have problems in the (30–30 kilo rad) dose range (Mahadeo et al. 2018). In this work, dose is obtained by

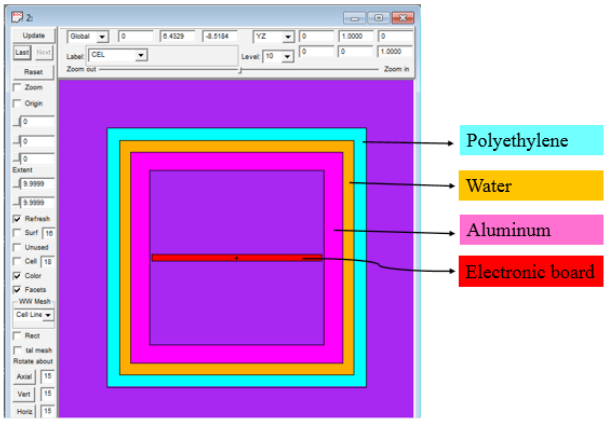

Fig. 2. Multi-layered structure designed in this work.

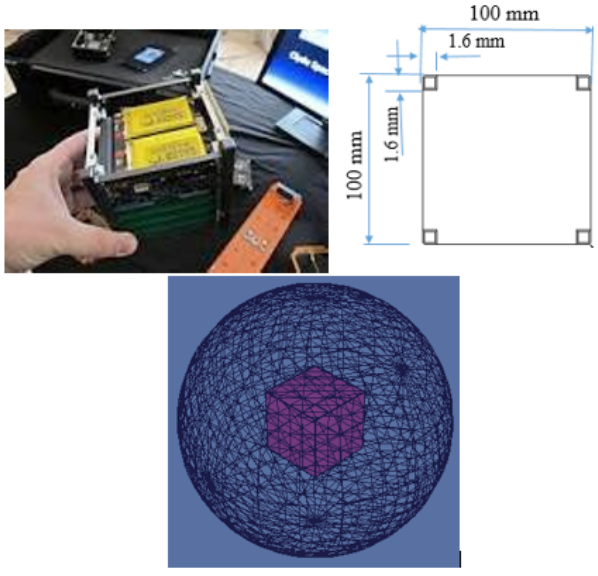

Fig. 3. 1.6 mm thick cube shield made by cube sat company, which is simulated by MCNPX code.

using Tally number (F6) with a suitable number of records which reduces the statistical error below 1%. The source energy distribution and probability have been calculated using the output obtained from SPENVIS for the mission, with the particle flux in each energy being considered as its probability.

Table 1 contains calculations of the dose caused by trapped particles in the MULLASSIS code based on changes in the thickness of aluminum and polyethylene. It can be seen that by changing the thickness of aluminum (reducing the thickness of aluminum) and adding polyethylene as the second layer for composite protection, the maximum absorption dose occurs in the protection layers at a thickness of 0.6 mm aluminum (Fig. 2). And in this case, the absorbed dose by the two-layer protection is 3.58 and 1.8 times, respectively, the absorbed dose by the aluminum and polyethylene layers alone.

According to the simulation results in MULLASSIS code (Fig. 4), it was found that for a box with a thickness of 1.6 mm, at a thickness of 0.6 mm for aluminum and 1 mm for polyethylene (mode G in Table 1), the highest absorption dose occurred and the most optimal thicknesses for the two-layer shield was determined by the mentioned values.

In the next step, by adding a middle layer of water, the simulations were performed in MCNP and MULLASSIS codes, and after checking the output of the software, it was found that the thickness of 0.55 mm for water as the middle layer and 0.45 mm for polyethylene as the last layer, the highest amount of absorbed dose was recorded in both codes (Figs. 5 and 6). Therefore, by examining the results, it

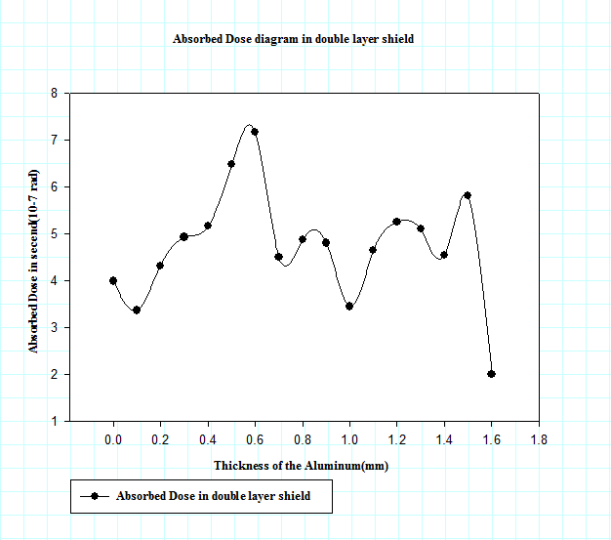

Fig. 4. Dose curve according to the thickness of the aluminum layer in the two-layer aluminum-polyethylene shield, where the total thickness of the shield is 1.6 mm.

wcan be concluded that the most optimal mode for a three-layer shield with a thickness of 1.6 mm is the simulation mode F in Table 2.

3. RESULTS

By comparing graphs (Figs. 5 and 6), we can conclude: firstly, the output of both simulations are consistent. Secondly, in the thicknesses of 0.45 mm for polyethylene

Table 1. Dose caused by trapped particles based on different thicknesses of two layers of protective layers

Total absorbed dose in second (10^{-7} *rad*)	Second layer (polyethylene)		First layer (aluminum)		Simulation mode
	Absorbed dose (10^{-7} *rad*)	Thickness (mm)	Absorbed dose (10^{-7} *rad*)	Thickness (mm)	
3.9887	3.9887	1.6	0.0000	0.0	A
3.3660	1.7927	1.5	1.5733	0.1	B
4.3132	2.3794	1.4	1.9338	0.2	C
4.9285	2.8688	1.3	2.0597	0.3	D
5.1644	2.7071	1.2	2.4573	0.4	E
6.4702	2.9964	1.1	1.4738	0.5	F
7.1725	4.2879	1.0	2.8846	0.6	G
4.4998	2.3030	0.9	2.1968	0.7	H
4.8700	2.7187	0.8	2.1513	0.8	I
4.8006	3.1567	0.7	1.6439	0.9	J
3.4442	1.9716	0.6	1.4726	1.0	K
4.6457	3.9342	0.5	2.7115	1.1	L
5.2429	3.4712	0.4	1.7717	1.2	M
5.1006	2.7460	0.3	2.3546	1.3	N
4.5487	2.6180	0.2	1.9307	1.4	O
5.8169	3.0447	0.1	2.7722	1.5	P
2.0019	0.0000	0.0	2.0019	1.6	Q

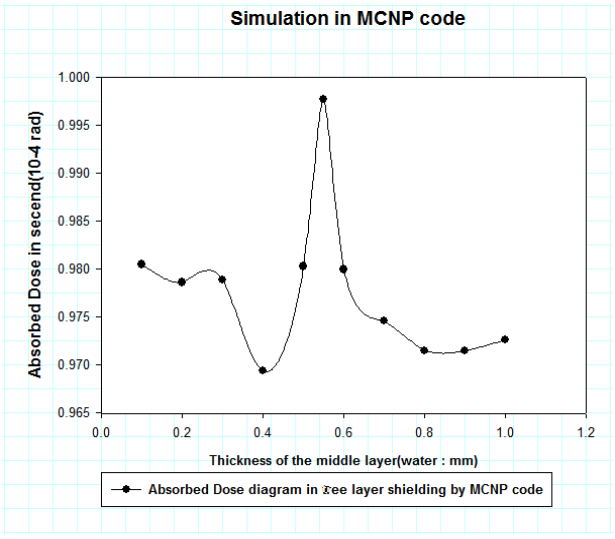

Fig. 5. Absorbed dose curve according to the thickness of the water layer (middle layer) in the aluminum-water-polyethylene three-layer shield in the MCNP code, where the total thickness of the shield (according to the simulation modes in Table 2) is 1.6 mm.

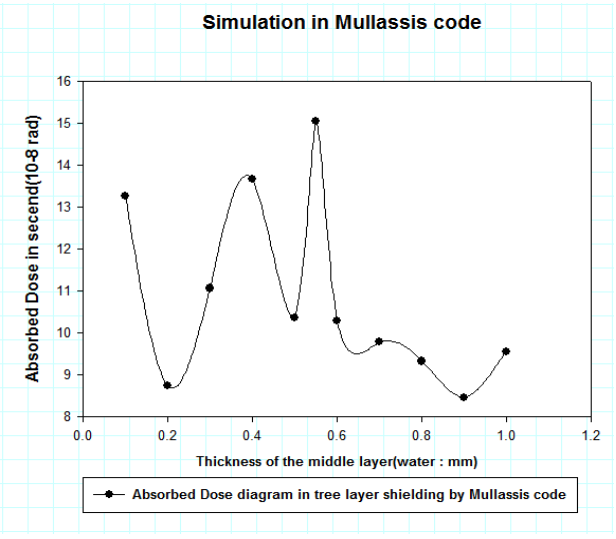

Fig. 6. Absorbed dose curve according to the thickness of the water layer (middle layer) in the aluminum-water-polyethylene three-layer shield in the MULLASSIS code, where the total thickness of the shield (according to the simulation Modes in Table 2) is 1.6 mm.

Table 2. Dose caused by trapped particles based on different thicknesses of three layers of protection layers in MCNP and MULLASSIS codes

MCNPX code	MULLASSIS code	Thickness of the last layer (polyethylene): (mm)	Thickness of the middle layer (water): (mm)	Thickness of the first layer (aluminum): (mm)	Simulation mode
Total absorbed dose in second (10^{-4} *rad*)	Total absorbed dose in second (10^{-8} *rad*)				
0.98047	13.2687	0.90	0.10	0.60	A
0.97859	08.7412	0.80	0.20	0.60	B
0.97885	11.0617	0.70	0.30	0.60	C
0.96935	13.6729	0.60	0.40	0.60	D
0.98026	10.3674	0.50	0.50	0.60	E
0.99776	15.0460	0.45	0.55	0.60	F
0.97994	10.2768	0.40	0.60	0.60	G
0.97457	09.7853	0.30	0.70	0.60	H
0.97146	09.3227	0.20	0.80	0.60	I
0.97143	08.4544	0.10	0.90	0.60	J
0.97256	09.5570	0.00	1.00	0.60	K

as the first layer of protection, 0.55 mm for water as the middle layer and 0.6 mm for aluminum as the inner layer of protection, the maximum absorbed dose was obtained and it was calculated to be approximately 2.09 times that of the two- layer protection mode.

In the design of the shield, it is attempted to make the thickness of the layers of materials with higher density as less as possible so that the mass of the shield is optimized. For this purpose, the number of available combination cases of different layer thicknesses have been considered which can be seen in Table 3. Taking the importance of mass into account and if installing electronic parts can be nonobligatory, the use of multi-layer protection is very effective in reducing the mass. Moreover, among all considered modes, having a higher attenuation than aluminum in reducing the mass, the F mode, which is the most favorable mode, has a mass reduction percentage of 39.69.

4. CONCLUSIONS

In order to reduce the destructive effects of space radiation on the electronic components of satellites or spacecraft, it is essential to use radiation shields. Meanwhile, shielding mass is an essential factor in designing the body of satellites. Accordingly, in this work, multi-layer shields made of polyethylene, water and aluminum were investigated to protect parts in space missions and compared with other common shield materials (such as aluminum). The results

Table 3. Thickness of layers of different materials in each of the cases considered for multi-layer shield

Discharged energy in the shield (Mev/g)	Total mass of the shield (kg)	Thickness of the last layer (polyethylene): (mm)	Thickness of the middle layer (water): (mm)	Thickness of the first layer (aluminum): (mm)	Simulation mode
1.093	0.25920	0.00	0.00	1.6	A
1.239	0.09600	0.00	1.60	0.0	B
1.507	0.08832	1.60	0.00	0.0	C
1.508	0.15360	1.00	0.00	0.6	D
1.446	0.15840	0.00	1.00	0.6	E
1.534	0.15630	0.45	0.55	0.6	F

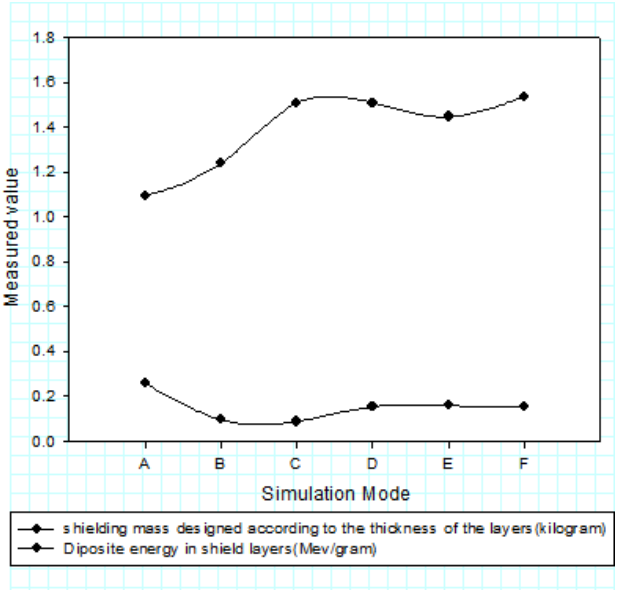

Fig. 7. Dose attenuation and mass reduction in different cases of three-layer shielding.

indicated that if there is no requirement to use single-layer aluminum boxes to place electronic components inside, the use of multi-layer shielding -introduced in this work- can reduce the absorbed dose of the shielding layers by 35.3% and 44.1% respectively, for double-layer shielding (aluminum, polyethylene) and three-layer (aluminum, water, polyethylene). In addition, this can be effective in protecting electronic components as well. It was also found out by calculations that the mass of the two-layer and three-layer shield was reduced by 38.88% and 39.69%, respectively, compared to the corresponding aluminum shield, and a lighter shield with better efficiency was designed (Fig. 7).

ACKNOWLEDGMENTS

The authors would like to acknowledge M.Askari for his guidance and advice carried us.

ORCIDs

Ali Alizadeh https://orcid.org/0009-0006-8841-2254
Gohar Rastegarzadeh https://orcid.org/0000-0001-9240-7841

REFERENCES

Arif Sazali M, Rashid NKA, Hamzah K, A review on multilayer radiation shielding, IOP Conf. Ser.: Mater. Sci. Eng. 555, 012008 (2019). https://doi.org/10.1088/1757-899X/555/1/012008

Blachowicz T, Ehrmann A, Shielding of cosmic radiation by fibrous materials, Fibers. 8, 60 (2021). https://doi.org/10.3390/fib9100060

Daneshvar H, Ghordoei Milan K, Sadr A, Sedighy SH, Malekie S, et al., Multilayer radiation shield for satellite electronic components protection, Sci. Rep. 11, 20657 (2021). https://doi.org/10.1038/s41598-021-99739-2

Ferrari A, Kiselev D, Koi T, Wohlmuther M, Davide JM, Po-production in lead: a benchmark between Geant4, FLUKA and MCNPX (2018) [Internet], viewed 2024 Feb 20, available from: https://arxiv.org/abs/1806.03732

Hussein KS, Electron, proton, and alpha stopping powers of polyvinyl toluene (PVT) scintillator crystal, IOP Conf. Ser.: Mater. Sci. Eng. 928, 072134 (2020). https://doi.org/10.1088/1757-899X/928/7/072134

ISISPACE, CubeSat structures (2024) [Internet], viewed 2024 Feb 20, available from: https://www.isispace.nl/product-category/cubesat-structures/

Lei P, Yang C, Zhang H, Liu C, Yan D, et al., Radiation shielding optimization design research based on bare-bones particle swarm optimization algorithm, Nucl. Eng. Technol. 55, 2215-2221 (2023). https://doi.org/10.1016/j.net.2023.02.018

Li H, Qin Y, Yang Y, Yao M, Wang X, et al., The evolution of interaction between grain boundary and irradiation-induced point defects: symmetric tilt GB in tungsten, J. Nucl. Mater. 500, 42-49 (2018). https://doi.org/10.1016/j.jnucmat.2017.12.013

Liu B, Lv H, Li L, Chai X, Xu H, et al., Multi-objective optimization design of radiation shadow shield for space nuclear power with genetic algorithm, Front. Energy Res. 10, 800930 (2022). https://doi.org/10.3389/fenrg.2022.800930-

Mahadeo DM, Rohwer LES, Martinez M, Nowlin RN, Assessment of commercial-off-the-shelf electronics for use in a shortterm geostationary satellite, Sandia National Laboratories Technical Report, No. SAND-2018-12254 (2018).

Narici L, Casolino M, Di Fino L, Larosa M, Picozza P, et al., Performances of kevlar and polyethylene as radiation shielding on-board the International Space Station in high latitude radiation environment, Sci. Rep. 7, 1644 (2017). https://doi.org/10.1038/s41598-017-01707-2

National Academies of Sciences, Engineering, and Medicine, Testing at the Speed of Light: The State of U.S. Electronic Parts Space Radiation Testing Infrastructure (The National Academies Press, Washington, 2018).

Nwankwo VUJ, Jibiri NN, Kio MT, The impact of space radiation environment on satellites operation in near-earth space, in Satellites Missions and Technologies for Geosciences, eds. Demyanow V, Becedas J (IntechOpen, London, 2020).

Rahman MM, Shankar D, Santra S, Analysis of radiation environment and its effect on spacecraft in different orbits, Proceedings of the International Astronautical Congress (IAC2017), Adelaide, Australia, 25–29 Sep 2017.

Rudychev VG, Azarenkov NA, Girka IO, Rudychev YV, Optimization of radiation shields made of Fe and Pb for the spent nuclear fuel transport casks, Nucl. Eng. Technol. 55, 690-695 (2023). https://doi.org/10.1016/j.net.2022.10.002

Seon J, Chae KS, Na GW, Seo HK, Shin YC, et al., Particle detector (PD) experiment of the Korea Space Environment Monitor (KSEM) aboard geostationary satellite GK2A, Space Sci. Rev. 216, 13 (2020). https://doi.org/10.1007/s11214-020-0636-4

Shoorian S, Jafari H, Feghhi SAH, Aslani G, Calculation and measurement of leakage current variations due to displacement damage for a silicon diode exposed to space protons, J. Space Sci. Technol. 13, 71-79 (2019). https://doi.org/10.30699/jsst.2021.1227

Sicard-Piet A, Bourdarie S, Boscher D, Friedel RHW, Thomsen M, et al., A new international geostationary electron model: IGE-2006, from 1 keV to 5.2 MeV, Space Weather. 6, S07003 (2008). https://doi.org/10.1029/2007SW000368

Tripathi Ram K, Active Space Radiation Shielding for Deep Space Missions (NASA Langley Research Center, Hampton, 2011).

Vepsäläinen AP, Karamlou AH, Orrell JL, Dogra AS, Loer B, et al., Impact of ionizing radiation on superconducting qubit coherence, Nature 584, 551-556 (2020). https://doi.org/10.1038/s41586-020-2619-8

Xu H, Sun W, Yan Y, Hu G, Hu H, Optimal shielding structure design for a typical 14 MeV neutron source, AIP Adv. 12, 035137 (2022). https://doi.org/10.1063/5.0078250